PROCEEDINGS OF SCIENCE

Measurement of cosmic rays with energies down to the PeV region using the TALE-infill SD array

Yusuke Kawachi[a,*] **on behalf of the Telescope Array Collaboration**

[a] *Graduate School of Science, Osaka Metropolitan University, 3-3-138, Sugimoto, Sumiyoshi-ku, Osaka, 558-8585, Japan*

E-mail: sd23481w@st.omu.ac.jp

The Telescope Array Low-energy Extension (TALE) experiment is a project that extends the Telescope Array (TA) experiment to observe cosmic rays with energies down to $10^{16.5}$ eV using 10 fluorescence detectors (FDs) and 80 surface detectors (SDs). The TALE-infill SD array, consisting of 50 SDs arranged in a grid pattern with 100-meter spacing, has been installed to extend observations to lower energies, covering the PeV energy region. The extension as TALE-infill enables precise measurements of the energy spectrum, mass composition, and arrival direction anisotropy of cosmic rays around the knee, with the aim of investigating the origin of cosmic rays and the physical mechanisms responsible for the knee feature. In this paper, we report on the observational status of the TALE-infill array, using the first data from November 2023 to Jun 2024.

7th International Symposium on Ultra High Energy Cosmic Rays (UHECR2024)
17-21 November 2024
Malargüe, Mendoza, Argentina

*Speaker

 ISSN 1824-8039 . Published by SISSA Medialab.

PoS(UHECR2024)096

1. Introduction

The cosmic ray energy spectrum exhibits the changing the spectrum index around the $10^{15.6}$ and 10^{17} eV, known as the knee and 2nd knee respectively, as shown in the left panel of Figure 1. One of the leading hypotheses is that the knee structure is caused by the acceleration limit of proton cosmic rays within the Milky Way. Since acceleration in a magnetic field is considered to be proportional to the atomic number of cosmic ray nuclei, it is expected that, beyond the acceleration limit energy, the mass composition of cosmic rays transitions from lighter nuclei to heavier nuclei in this energy range. The results of mass composition measurements from various experiments indeed show a trend of transitioning to heavier masses beyond the knee. However, as shown in the right panel of Figure 1, the absolute values measured in different experiments exhibit significant differences that exceed the errors representative of their distributions. To clarify the origin and mechanism of the knee, it is important to accurately measure the energy spectrum and mass composition of cosmic rays in the knee region, which is defined as approximately 1 PeV to 10 PeV.

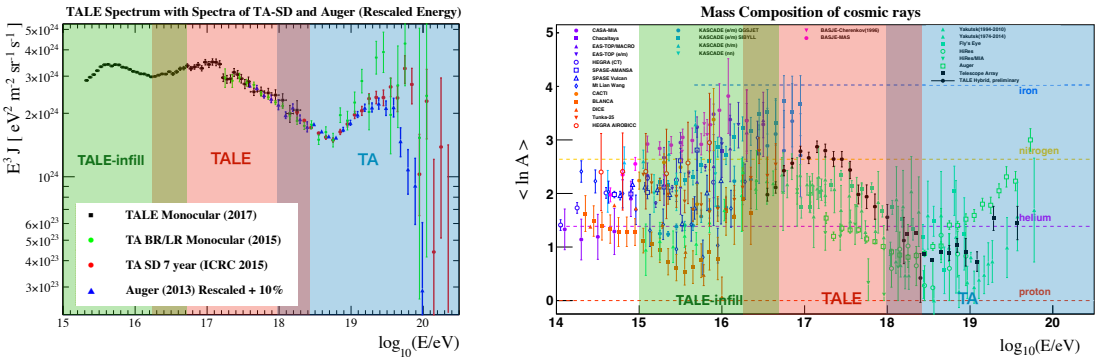

Figure 1: Left : The energy spectrum of cosmic rays measured by the TA experiment. The spectrum has breaks at $10^{15.6}$ and 10^{17} eV. Right : The average mass of cosmic rays measured by various experiments [2–26]. There is a large variation in the results with several experiments has large uncertainties. The area shaded in blue represents the observation range of TA. The red area is TALE's observation range. The green area shows the observation range of TALE-infill.

The Telescope Array (TA) experiment started the Telescope Array Low-energy Extension (TALE) to observe cosmic rays below 10^{18} eV. The TALE detectors are located at the northwest part of the TA site. Since 2018, we started data taking with 10 fluorescence detectors (FDs) and an SD array covering an area of 21 km^2. The TALE SD array comprises 80 plastic scintillation detectors, with 40 arranged at 400 m intervals and the remaining 40 at 600 m intervals, as illustrated in Figure 2a. To further extend the observational range of TALE to lower energies and to investigate cosmic rays in the knee region, a higher-density SD array than the TALE SD array—referred to as the TALE-infill SD array—has been deployed. This array is located between the TALE FD and the TALE SD array and consists of 50 SDs arranged in a rectangular grid with 100 m spacing (Figure 2b). Air shower events are triggered when five or more adjacent SDs record signals exceeding 3 MIPs within a time window of 3 μs . The TALE-infill SD array began operation in November 2023 and has been operating stably since then. An example of air shower event recorded by TALE-infill SD is shown in Figure 3.

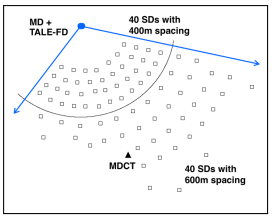

(a) The TALE SD

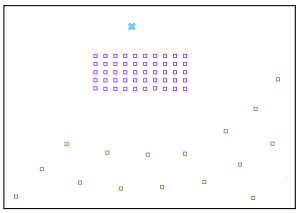

(b) The TALE-infill SD

Figure 2: (a) A map of TALE. The blue circle (•) and arrows (→) represent TALE FD and it's field of view. The open square boxes (□) shows TALE SDs. (b) Detector configuration of the TALE-infill SD. The purple square boxes (□), cyan cross mark (×) and green square boxes (□) correspond to TALE-infill SD, TALE FD and TALE SD respectively.

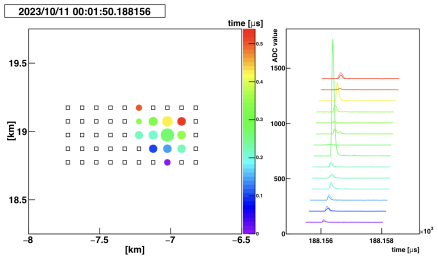

Figure 3: The shower foot print (left) and the signal waveforms (right) of an event obtained by the TALE-infill SD arrray. The size of the circles is proportional to the number of detected particles. The color represents the relative trigger times.

2. Reconstruction method

The reconstruction of air showers detected by the TALE-infill SD array begins with noise rejection, where spatial and temporal clustering algorithms remove isolated signals such as single muon hits to ensure that only shower-induced signals are used. Following this, the initial geometry of the air shower is determined by fitting the timing data of clustered SDs to a modified Linsley shower-shape time delay function [30, 31] as given below.

$$\tau = (8 \times 10^{-10}) a(\theta) \left(1.0 + \frac{r}{30}\right)^{1.5} \rho^{-0.5} \text{ [s]} \tag{1}$$

$$a(\theta) = \begin{cases} 3.3836 - 0.01848\theta & (\theta < 25^\circ) \\ c_0 + c_1\theta + c_2\theta^2 + c_3\theta^3 & (25^\circ \leq \theta \leq 35^\circ) \\ \exp\left(-3.2 \times 10^{-2}\theta + 2.0\right) & (35^\circ < \theta) \end{cases} \tag{2}$$

$$c_0 = -7.76168 \times 10^{-2}, \quad c_1 = 2.99113 \times 10^{-1}$$
$$c_2 = -8.79358 \times 10^{-3}, \quad c_3 = 6.51127 \times 10^{-5}$$

Here, τ [s] is the delay time from the shower plane, r [m] is the distance from the shower axis, ρ [m^{-2}] is the particle number density and $a(\theta)$ represents the curvature of the air shower front, where θ is the zenith angle . Next, the lateral distribution of particle densities at the ground is fitted using the NKG function [32, 33] in Equation (3).

$$\rho^{\text{FIT}} = N \left(\frac{r}{R_M}\right)^{s-2} \left(1 + \frac{r}{R_M}\right)^{s-4.5} \text{ [m}^{-2}\text{]} \tag{3}$$

where N [m^{-2}] is the scale factor, R_M [m] is the Molière radius and s is the shower age. Examples of the geometry fit and LDF fit for a event are shown in Figure 4 and Figure 5, respectively. To further refine the reconstruction, the procedure is iterated: the geometry fit is repeated using the results from the lateral fit as the initial values, followed by another lateral fit.
This iterative process—geometry fit, lateral fit, geometry fit, and lateral fit—serves to progressively improve the accuracy of both the arrival direction and the core position.

From the final lateral fit, the shower size parameter s_{50}, defined as the particle density at 50 m from the shower axis, is obtained. The energy of the primary cosmic ray is estimated using an energy lookup table generated with QGSJETII-04 [35] proton showers (refer to Figure 6). This table provides the energy corresponding to a given s_{50} value and reconstructed zenith angle.

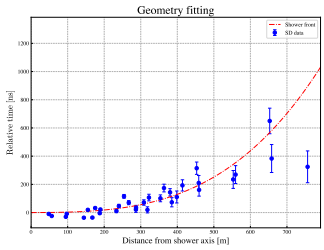

Figure 4: An example of the geometry fitting. The blue dots represent the trigger times of SDs and the red dashed line is the fit result.

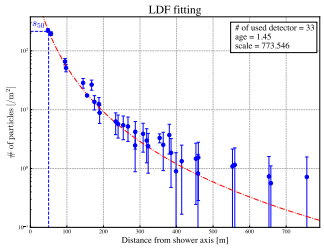

Figure 5: An example of the LDF fitting. The blue dots represent the signals in MIP recorded by SDs. The dashed line is the fit result.

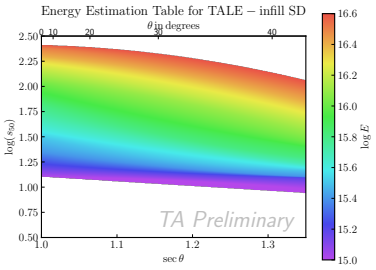

Figure 6: The energy estimation table for TALE-infill. In this study, this table was created under the assumption that all primary cosmic rays are protons.

3. Resolution

We evaluated the reconstruction performance of the TALE-infill SD array using simulations. In this study, we use a set of air showers generated by the CORSIKA air shower simulation tool with the QGSJETII-04 [35] interaction model. For the detector simulation, we use the GEANT4 [36] based simulation originally developed by the TA SD simulation. The Monte Carlo (MC) dataset conditions are shown in Table 1.

Table 1: MC dataset

Primary particle	proton
MC simulation	CORSIKA
Had. interaction model	QGSJETII-04
Energy E	$10^{15.7}$ eV $\sim 10^{16.5}$ eV
Zenith angle θ	$0° \leq \theta \leq 65°$, ($\propto \sin\theta\cos\theta$)
Azimuth angle ϕ	$0° \leq \phi \leq 360°$, uniformly
Core position	Uniformly random within a circle of radius 1 km from the array center

We evaluate the performance of TALE-infill SD array by using the MC simulations described in Table 1. We removed bad events by using the quality cuts shown below.

- The number of SDs used in reconstruction is 10 or fewer
- Reconstructed zenith angle is greater than 45°
- Reconstructed core position is outside the array
- The SD with the maximum signal in an event is located on the edge of the array
- The distance from the reconstructed core position to the signal barycenter is 200 m or more
- The age parameter (s) of the LDF fit falls outside the range of 0.2 to 1.9
- The distance between the shower axis and the closest SD used in the LDF fit is 70 m or more

Figure 7 shows the comparison of the simulated and reconstructed parameters. The core position resolution is about 5 m, the angular resolution is approximately 1.5 degrees and the energy resolution is around 30% at 10^{16} eV. We also checked the angular resolution by analyzing the

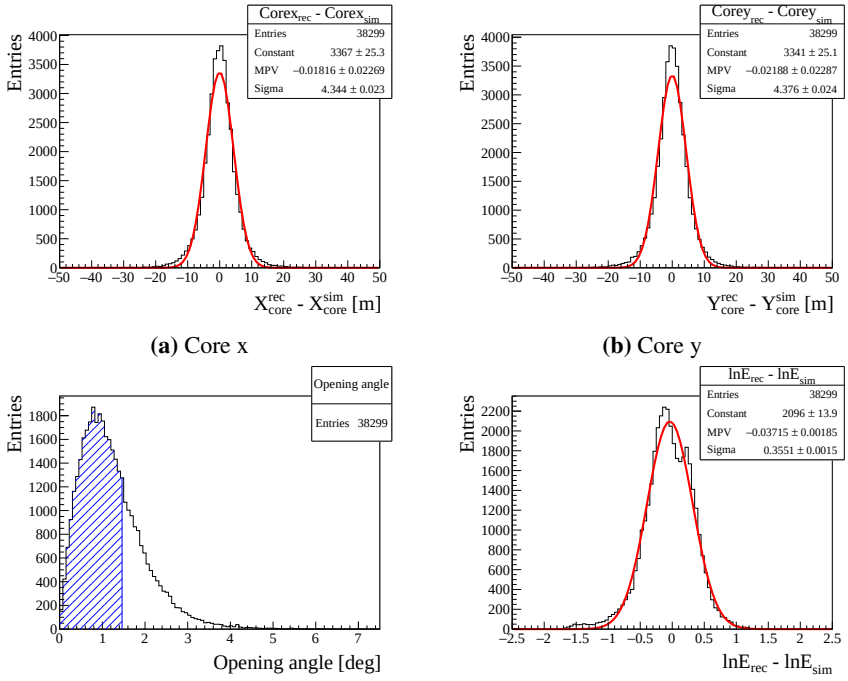

(a) Core x **(b)** Core y

(c) Arrival direction **(d)** Energy

Figure 7: TALE-infill SD array resolution. (a)(b) The distance from the true core position to the reconstructed core position for x coordinate (a) and y coordinate (b). The red lines show the result of gaussian fitting. (c) The opening angle between the true arrival direction and the reconstructed direction. The blue area contains 68% of all reconstructed events which passed the quality cuts. The 68% region is within 1.44 degrees. (d) The difference in simulated and reconstructed energy.

observation data from November 2023 to January 2024 with the even-odd method [38]. In this method, we divided the TALE-infill SD array into odd and even subarrays. Each subarray consists of 25 SDs. Adjacent SDs in the original array are assigned to different subarrays, and the spacing between SDs in the subarrays is 141 m. We reconstructed events using both subarrays and computed the distribution of opening angles between the reconstructed arrival directions. Figure 8 shows the opening angle distribution obtained from the even-odd method. The angular resolution of the full-size array is defined as half of the opening angle, which in this case is $3.14/2 \approx 1.5$. This

result is consistent with the resolution obtained from MC simulations, confirming the capability of he MCs to replicate experimental events.

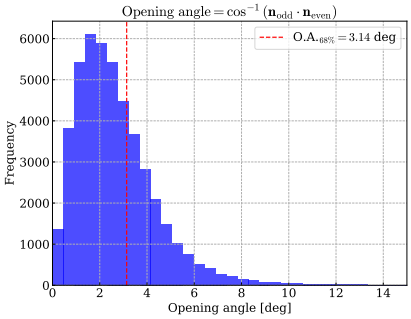

Figure 8: The opening angle distribution from real events reconstructed using the even-odd method. The red dashed line indicates the 68% value, which is 3.14 degrees. In the analysis using all SDs, the angular resolution is half of this value, 1.57 degrees.

4. Data/MC comparison

We compared the experimental data distributions with the MC distributions for the main reconstructed parameters. The results are shown in Figure 9. The black points represent the experimental data. The red histograms show the MC expectation. The experimental data and MC results are in general agreement; however, the distribution of the number of SDs used in the reconstruction exhibits a noticeable discrepancy at higher SD counts.

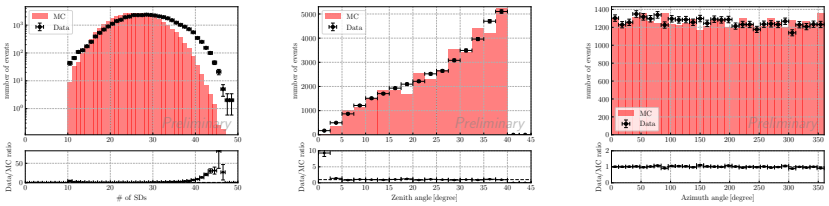

(a) # of SDs **(b)** Zenith angle θ [degree] **(c)** Azimuth angle ϕ [degree]

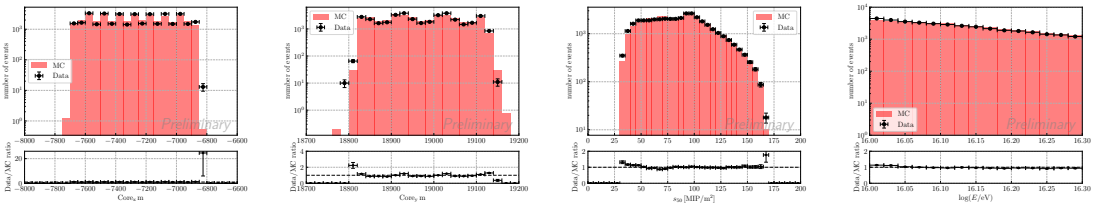

(d) Core x [m] **(e)** Core y [m] **(f)** s_{50} [MIP/m^2] **(g)** $\log(E/\mathrm{eV})$

Figure 9: Data/MC comparison. It comparisons shows agreement except for the # of SDs.

5. Conclution and outlook

In summary, the TALE-infill SD array has been installed to observe cosmic rays from the knee region and above. We developed simulation code and the reconstruction program for the TALE-infill SD array. The resolution of the reconstructed shower is approximately 5 m for the air shower core position, about 1.5° for the arrival direction, and around 30% for the cosmic ray energy determination. We confirmed that the angular resolution from the MC analysis is consistent with the one obtained from the observational data using the even-odd method. After comparing 8 months of data with the MC simulations, we found that all distributions except for the number of detectors were consistent. Future work will look to resolve this disagreement and extend the analysis down to the knee region.

References

[1] G.V. Kulikov and G.B. Khristiansen, *Soviet Physics JETP* **35** (1959) 441.

[2] M.A.K. Glasmacher et al., in *26th International Cosmic Ray Conference* (1999).

[3] C. Aguirre et al., *Phys. Rev. D* **62** (2000) 032003.

[4] C. Aguirre, H. Aoki, K. Hashimoto, K. Honda, N. Inoue, N. Kawasumi, Y. Maeda, N. Martinic, T. Matano, N. Ohmori et al., *Phys. Rev. D* **62** (2000) 032003.

[5] M. Aglietta et al. (EAS-TOP), *Astropart. Phys.* **21** (2004) 583.

[6] K. Bernlohr, W. Hofmann, G. Leffers, V. Matheis, M. Panter, R. Zink, *Astropart. Phys.* **8** (1998) 253.

[7] K. Rawlins (SPASE, AMANDA), in *28th International Cosmic Ray Conference* (2003).

[8] J.E. Dickinson et al., in *26th International Cosmic Ray Conference* (1999).

[9] M. Cha et al., in *27th International Cosmic Ray Conference* (2001).

[10] S. Paling et al., in *25th International Cosmic Ray Conference* (1997).

[11] J.W. Fowler, L.F. Fortson, C.C.H. Jui, D.B. Kieda, R.A. Ong, C.L. Pryke, P. Sommers, *Astropart. Phys.* **15** (2001) 49.

[12] S.P. Swordy, D.B. Kieda, *Astropart. Phys.* **13** (2000) 137.

[13] D. Chernov et al., *Int. J. Mod. Phys. A* **20** (2006) 6799.

[14] F. Arqueros et al. (HEGRA), *Astron. Astrophys.* **359** (2000) 682.

[15] T. Antoni et al. (KASCADE), *Astropart. Phys.* **24** (2005) 1.

[16] J. Horandel et al., in *16th European Cosmic Ray Symposium* (1998).

[17] T. Antoni et al. (KASCADE), *Astropart. Phys.* **16** (2002) 245.

[18] Y. Shirasaki et al., *Astropart. Phys.* **15** (2001) 357.

[19] S. Ogio et al., in *28th International Cosmic Ray Conference* (2003).

[20] S. Knurenko and A. Sabourov, *Astrophys. Space Sci. Trans.* **7** (2011) 251.

[21] S. Knurenko and A. Sabourov, *Advances in Space Research* **64** (2019) 2570-2577.

[22] D.J. Bird et al. (HiRes), *Astrophys. J.* **424** (1994) 491.

[23] R.U. Abbasi et al. (HiRes), *Astrophys. J.* **622** (2005) 910.

[24] T. Abu-Zayyad et al. (HiRes-MIA), *Astrophys. J.* **557** (2001) 686.

[25] M. Unger (Pierre Auger), *Astron. Nachr.* **328** (2007) 614.

[26] R.U. Abbasi et al. (Telescope Array), *The Astrophysical Journal* **858** (2018) 76.

[27] **Telescope Array** collaboration, K. Fujita, *PoS* **ICRC2023** (2023) 401.

[28] **Telescope Array** Collaboration, K. Fujita, *PoS* **UHECR2024** (2025) 042.

[29] **Telescope Array** Collaboration, I. Komae, *PoS* **ICRC2023** (2023) 405.

[30] Linsley, John and Scarsi, Livio, *Phys. Rev.* **128** (1962) 2384–2392.

[31] Teshima, M. and others, *J. Phys. G* **12** (1986) 1097.

[32] Kamata, Koichi and Nishimura, Jun, *Prog. Theor. Phys. Suppl.*, **6** (1958) 93–155.

[33] Greisen, K., *Ann. Rev. Nucl. Part. Sci.* **10** (1960) 63–108.

[34] B.T. Stokes et al., *Astropart. Phys.* **35** (2012) 759-766.

[35] S. Ostapchenko, *Phys. Rev. D* **83** (2011) 014018.

[36] S. Agostinelli et al., *Nucl. Instrum. Methods Phys. Res. A* **506** (2003) 250.

[37] Heck, D. and Knapp, J. and Capdevielle, J. N. and Schatz, G. and Thouw, T., *Nucl. Instrum. Methods Phys. Res. A* **506** (2003) 250.

[38] S.C. Tonwar, Workshop on Techniques in UHE -ray Astronomy, La Jolla, Eds: R.J. Protheroe S.A. Stephens, Univ. of Adelaide (1985) 40.

Full Authors List: The Telescope Array Collaboration

R.U. Abbasi[1], T. Abu-Zayyad[1,2], M. Allen[2], J.W. Belz[2], D.R. Bergman[2], I. Buckland[2], W. Campbell[2], B.G. Cheon[3], K. Endo[4], A. Fedynitch[5,6], T. Fujii[4,7], K. Fujisue[5,6], K. Fujita[5], M. Fukushima[5], G. Furlich[2], Z. Gerber[2], N. Globus[8*], W. Hanlon[2], N. Hayashida[9], H. He[8†], K. Hibino[9], R. Higuchi[8], D. Ikeda[9], T. Ishii[10], D. Ivanov[2], S. Jeong[11], C.C.H. Jui[2], K. Kadota[12], F. Kakimoto[9], O. Kalashev[13], K. Kasahara[14], Y. Kawachi[4], K. Kawata[5], I. Kharuk[13], E. Kido[8], H.B. Kim[3], J.H. Kim[2], J.H. Kim[2‡], S.W. Kim[11§], R. Kobo[4], I. Komae[4], K. Komatsu[15], K. Komori[16], C. Koyama[5], M. Kudenko[13], M. Kuroiwa[15], Y. Kusumori[16], M. Kuznetsov[13,17], Y.J. Kwon[18], K.H. Lee[3], M.J. Lee[11], B. Lubsandorzhiev[13], J.P. Lundquist[2,19], A. Matsuzawa[15], J.A. Matthews[2], J.N. Matthews[2], K. Mizuno[15], M. Mori[16], M. Murakami[16], S. Nagataki[8], M. Nakahara[4], T. Nakamura[20], T. Nakayama[15], Y. Nakayama[16], T. Nonaka[5], S. Ogio[5], H. Ohoka[5], N. Okazaki[5], M. Onishi[5], A. Oshima[21], H. Oshima[5], S. Ozawa[22], I.H. Park[11], K.Y. Park[3], M. Potts[2], M. Przybylak[23], M.S. Pshirkov[13,24], J. Remington[2¶], C. Rott[2,11], G.I. Rubtsov[13], D. Ryu[25], H. Sagawa[5], N. Sakaki[5], R. Sakamoto[16], T. Sako[5], N. Sakurai[5], S. Sakurai[4], D. Sato[15], S. Sato[16], K. Sekino[5], T. Shibata[5], J. Shikita[4], H. Shimodaira[5], B.K. Shin[25], H.S. Shin[4,7], K. Shinozaki[26], J.D. Smith[2], P. Sokolsky[2], B.T. Stokes[2], T.A. Stroman[2], Y. Takagi[16], K. Takahashi[5], M. Takeda[5], R. Takeishi[5], A. Taketa[27], M. Takita[5], Y. Tameda[16], K. Tanaka[28], M. Tanaka[29], S.B. Thomas[2], G.B. Thomson[2], P. Tinyakov[13,17], I. Tkachev[13], T. Tomida[15], S. Troitsky[13], Y. Tsunesada[4,7], S. Udo[9], F. Urban[30], I.A. Vaiman[13‖], M. Vrabel[26], D. Warren[8], K. Yamazaki[21], Y. Zhezher[5,13], Z. Zundel[2], and J. Zvirzdin[2]

[1] *Department of Physics, Loyola University Chicago, Chicago, Illinois 60660, USA*
[2] *High Energy Astrophysics Institute and Department of Physics and Astronomy, University of Utah, Salt Lake City, Utah 84112-0830, USA*
[3] *Department of Physics and The Research Institute of Natural Science, Hanyang University, Seongdong-gu, Seoul 426-791, Korea*
[4] *Graduate School of Science, Osaka Metropolitan University, Sugimoto, Sumiyoshi, Osaka 558-8585, Japan*
[5] *Institute for Cosmic Ray Research, University of Tokyo, Kashiwa, Chiba 277-8582, Japan*
[6] *Institute of Physics, Academia Sinica, Taipei City 115201, Taiwan*
[7] *Nambu Yoichiro Institute of Theoretical and Experimental Physics, Osaka Metropolitan University, Sugimoto, Sumiyoshi, Osaka 558-8585, Japan*
[8] *Astrophysical Big Bang Laboratory, RIKEN, Wako, Saitama 351-0198, Japan*
[9] *Faculty of Engineering, Kanagawa University, Yokohama, Kanagawa 221-8686, Japan*
[10] *Interdisciplinary Graduate School of Medicine and Engineering, University of Yamanashi, Kofu, Yamanashi 400-8511, Japan*
[11] *Department of Physics, Sungkyunkwan University, Jang-an-gu, Suwon 16419, Korea*
[12] *Department of Physics, Tokyo City University, Setagaya-ku, Tokyo 158-8557, Japan*
[13] *Institute for Nuclear Research of the Russian Academy of Sciences, Moscow 117312, Russia*
[14] *Faculty of Systems Engineering and Science, Shibaura Institute of Technology, Minato-ku, Tokyo 337-8570, Japan*
[15] *Academic Assembly School of Science and Technology Institute of Engineering, Shinshu University, Nagano, Nagano 380-8554, Japan*
[16] *Graduate School of Engineering, Osaka Electro-Communication University, Neyagawa-shi, Osaka 572-8530, Japan*
[17] *Service de Physique Theorique, Universite Libre de Bruxelles, Brussels 1050, Belgium*
[18] *Department of Physics, Yonsei University, Seodaemun-gu, Seoul 120-749, Korea*
[19] *Center for Astrophysics and Cosmology, University of Nova Gorica, Nova Gorica 5297, Slovenia*
[20] *Faculty of Science, Kochi University, Kochi, Kochi 780-8520, Japan*
[21] *College of Science and Engineering, Chubu University, Kasugai, Aichi 487-8501, Japan*
[22] *Quantum ICT Advanced Development Center, National Institute for Information and Communications Technology, Koganei, Tokyo 184-8795, Japan*
[23] *Doctoral School of Exact and Natural Sciences, University of Lodz, Lodz, Lodz, 90-237, Poland*
[24] *Sternberg Astronomical Institute, Moscow M.V. Lomonosov State University, Moscow 119991, Russia*
[25] *Department of Physics, School of Natural Sciences, Ulsan National Institute of Science and Technology, UNIST-gil, Ulsan 689-798, Korea*
[26] *Astrophysics Division, National Centre for Nuclear Research, Warsaw 02-093, Poland*
[27] *Earthquake Research Institute, University of Tokyo, Bunkyo-ku, Tokyo 277-8582, Japan*
[28] *Graduate School of Information Sciences, Hiroshima City University, Hiroshima, Hiroshima 731-3194, Japan*
[29] *Institute of Particle and Nuclear Studies, KEK, Tsukuba, Ibaraki 305-0801, Japan*
[30] *CEICO, Institute of Physics, Czech Academy of Sciences, Prague 182 21, Czech Republic*

[*] Presently at: KIPAC, Stanford University, Stanford, CA 94305, USA
[†] Presently at: Purple Mountain Observatory, Nanjing 210023, China
[‡] Presently at: Physics Department, Brookhaven National Laboratory, Upton, NY 11973, USA
[§] Presently at: Korea Institute of Geoscience and Mineral Resources, Daejeon, 34132, Korea
[¶] Presently at: NASA Marshall Space Flight Center, Huntsville, Alabama 35812, USA
[‖] Presently at: Gran Sasso Science Institute, 67100 L'Aquila, L'Aquila, Italy